

Abstract

Understanding the temporal and spatial variation of wetland methane emissions is essential to the estimation of the global methane budget. We examine the seasonal and inter-annual variability in wetland methane emissions simulated in the Community Land Model (CLM4Me'). Methane emissions from both the Carbon-Nitrogen (CN, i.e. CLM4.0) and the Biogeochemistry (BGC, i.e. CLM4.5) versions of the CLM are evaluated. We further conduct simulations of the transport and removal of methane using the Community Atmosphere Model (CAM-chem) model using CLM4Me' methane emissions from both CN and BGC along with other methane sources and compare model simulated atmospheric methane concentration with observations. In addition, we simulate the atmospheric concentrations based on the TransCom wetland and rice paddy emissions from a different terrestrial ecosystem model VISIT. Our analysis suggests CN wetland methane emissions are higher in tropics and lower in high latitudes than BGC. In CN, methane emissions decrease from 1993 to 2004 while this trend does not appear in the BGC version. In the CN versions, methane emission variations follow satellite-derived inundation wetlands closely. However, they are dissimilar in BGC due to its different carbon cycle. CAM-chem model simulations with CLM4Me' methane emissions suggest that both prescribed anthropogenic and predicted wetlands methane emissions contribute substantially to seasonal and inter-annual variability in atmospheric methane concentration. It also suggests that different spatial patterns of wetland emissions can have significant impacts on N-S atmospheric CH₄ concentration gradients and growth rates. This study suggests that large uncertainties still exist in terms of spatial patterns and magnitude of global wetland methane budgets, and that substantial uncertainty comes from the carbon model underlying the methane flux modules.

Seasonal and inter-annual variability in wetland methane emissions

L. Meng et al.

Title Page

Abstract

Introduction

Conclusions

References

Tables

Figures



Back

Close

Full Screen / Esc

Printer-friendly Version

Interactive Discussion



1 Introduction

The increase in atmospheric methane (CH_4) concentration since 2007 (Rigby et al., 2008) has received attention due to methane's strong greenhouse effect. The causes of the renewed increase in CH_4 since 2007 and the relative stability of the atmospheric concentrations for the preceding decade (1996–2006) are not well understood (Bloom et al., 2010). Improved understanding of the variability of atmospheric methane can provide more accurate predictions of future concentrations. Changes in atmospheric CH_4 are determined by the balance between the emissions of CH_4 and its loss. The loss is mostly controlled by the reaction of CH_4 with the hydroxyl radical (OH). While the CH_4 loss timescale varies from year to year (Bousquet et al., 2006; Wuebbles and Hayhoe, 2002) as the OH concentration changes, recent evidence suggests the interannual variability of OH is small (Montzka et al., 2011). The primary sources of atmospheric methane include anthropogenic emissions, natural wetlands, rice paddies, biomass burning, and termites (Denman et al., 2007; Kirschke et al., 2013). Natural wetlands are the largest single source of atmospheric CH_4 and make a significant contribution to its variability (Spahni et al., 2011). Using inverse methods Bousquet et al. (2006) suggests that 70% of the global emission anomalies CH_4 for the period 1984–2003 are due to the inter-annual variability in wetland emissions and furthermore that tropical methane emissions are the dominant contribution to the global inter-annual variability. In another methane inversion, Chen and Prinn (2006) find that the large 1998 increase in atmospheric CH_4 concentration could be attributed to global wetland emissions.

There are still large uncertainties in global wetland emissions due to (1) poor understanding of environmental and biological processes that control methane emissions (Meng et al., 2012; Riley et al., 2011); and (2) uncertainties in extent and distribution of wetlands, particularly in tropical region (Prigent et al., 2007; Spahni et al., 2011). Process-based biogeochemical methane models can help improve the understanding of dominant processes that control methane production, oxidation, and transport.

BGD

12, 2161–2212, 2015

Seasonal and inter-annual variability in wetland methane emissions

L. Meng et al.

Title Page

Abstract

Introduction

Conclusions

References

Tables

Figures



Back

Close

Full Screen / Esc

Printer-friendly Version

Interactive Discussion



largest contribution to global wetland methane emissions (Bloom et al., 2010; Meng et al., 2012; Spahni et al., 2011).

The spatial distribution of surface emissions produced by these biogeochemical models can be used along with other CH₄ emission sources as inputs to atmospheric chemistry and transport models to simulate atmospheric CH₄ concentration. As wetland emissions are the largest single source, their spatial distribution could significantly affect the distribution of atmospheric CH₄ concentration. The long-term atmospheric measurement of CH₄ can be used to compare with modeled atmospheric CH₄ to further evaluate the spatial distribution of surface emissions. Recently, a chemistry-transport model (CTM) intercomparison experiment (TransCom-CH₄) quantifies the role of CH₄ surface emission distributions in simulating the global distribution of atmospheric methane (Patra et al., 2011). In TransCom-CH₄, twelve chemistry-transport models simulations with different surface emissions are evaluated against measured atmospheric CH₄ concentrations. Patra et al. (2011) find that meteorological conditions and surface emissions from biomass burning and wetlands can contribute up to 60% of the inter-annual variation (IAV) in the atmospheric CH₄ concentrations.

In this study, we explore the temporal and spatial variation of wetland methane emissions estimated in the CLM4Me'. The modeled wetland emissions are used with other surface emissions (including emissions from anthropogenic sources, biomass burning, rice paddies, and termites) as inputs to the Community Atmospheric Model with chemistry (CAM-chem). The CH₄ concentration simulated with CAM-chem is compared with a global network of station measurements. The purposes of this paper are (1) to examine seasonal and interannual variations in wetland methane emissions simulated by CLM4Me' in different versions of the Community Land Model; (2) to evaluate the relative importance of different surface emissions distributions of methane on the seasonal and inter-annual variations in atmospheric concentrations. Section 2 describes models, methods and datasets. Results and discussions are presented in Sect. 3. We conclude in Sect. 4 with a summary of major findings.

BGD

12, 2161–2212, 2015

Seasonal and inter-annual variability in wetland methane emissions

L. Meng et al.

Title Page

Abstract

Introduction

Conclusions

References

Tables

Figures

◀

▶

◀

▶

Back

Close

Full Screen / Esc

Printer-friendly Version

Interactive Discussion



2 Models and datasets

2.1 Simulations

Methane emissions from 1993–2004 are simulated and analyzed in four different model configurations (see Table 1). All configurations use Community Atmospheric Model (CAM4) with chemistry (CAM-chem) (Lamarque et al., 2012) to diagnose atmospheric methane. These configurations differ in their specification of methane emissions. Other details of the simulations are identical.

The TransCom simulation (Table 1) is reported on as part of the TransCom-CH₄ simulations (Patra et al., 2011). The CAM-chem model is one of the twelve models participating in these simulations (Patra et al., 2011). The methane emissions in the TransCom are specified and included the seasonal variation of methane emissions from anthropogenic sources (Olivier and Berdowski, 2001), rice paddies and wetlands (Ito and Inatomi, 2012), biomass burning (van der Werf et al., 2006), and termites Fung et al., 1991). The wetland emissions from Ito and Inatomi (2012) are calculated based on a process-based terrestrial ecosystem model, the Vegetation Integrative Simulator for Trace gases (VISIT). In the VISIT, the inundated area is calculated based on model-derived rainfall and temperature (Mitchell and Jones, 2005). We select this scenario from the TransCom experiment because it includes the long-term monthly variations of wetland and rice paddy emissions.

Differences between the TransCom simulation and the other three simulations analyzed here (see Table 1) include: (1) differences in the specification of the methane emissions from rice paddies and wetlands: in the TransCom simulation the emissions are specified while in the remaining three simulations the methane emissions are obtained from CLM4Me' a process-based methane biogeochemical model; (2) differences in the specification of fire emissions: in the TransCom simulation fire emissions are taken from Global Fire Emission Database (GFED) version 2 (on average 20 Tg CH₄ yr⁻¹ is emitted) (van der Werf et al., 2006) while in the remaining three sim-

BGD

12, 2161–2212, 2015

Seasonal and inter-annual variability in wetland methane emissions

L. Meng et al.

Title Page

Abstract

Introduction

Conclusions

References

Tables

Figures

⏪

⏩

◀

▶

Back

Close

Full Screen / Esc

Printer-friendly Version

Interactive Discussion



ulations the fire emissions are from GFED version 3 (on average 21.1 Tg CH₄ yr⁻¹ emitted) (Giglio et al., 2010).

Two of the configurations analyzed (labeled: CN_a and CN_b) diagnose wetlands and rice paddies methane emissions using CLM4Me' within the Community Land Model version 4 (CLM4 or CLM-CN) of the Community Earth System Model (CESM); one configuration (labeled BGC) uses CLM4Me' within the Community Land Model version 4.5 (CLM4.5 or CLM-BGC) of the CESM.

The wetland emissions simulated by the CLM4Me' model when integrated in the CLM4.0 are on the high side of the current estimates (Denman et al., 2007; Kirschke et al., 2013). In order to obtain a reasonable overall methane budget we adjust the emissions in the simulations using CLM4.0. In simulation CN_a the anthropogenic emissions used in the TransCom simulations are multiplied by 0.72; in simulation CN_b the wetland emissions are multiplied by 0.64, but the anthropogenic emissions are the same as those in TransCom. Both these rescalings retain the temporal and spatial emission distributions from the original datasets but simulate the approximately correct atmospheric methane concentrations. In the first case (CN_a), where anthropogenic emissions are reduced, the total anthropogenic emissions are 217 Tg yr⁻¹. This is at the low end of estimated anthropogenic emissions, but within the range (209–273 Tg) report of values in the literature (see IPCC AR4 Chapter 7) (Denman et al., 2007; Kirschke et al., 2013) when excluding biomass burning and rice paddies.

On the other hand the wetland emissions simulated by the CLM4Me' model integrated into CLM4.5 (BGC) are higher than the CLM4.0 (CN) emissions. Therefore, we adjust the wetland emissions in the BGC simulation. In particular in the BGC simulation the wetland emissions are reduced by 0.74 to match the total methane emissions in the other simulations. Reducing the methane emissions is equivalent to modifying the coefficient for the maximum amount of methane that can be produced from heterotrophic respiration. The reductions used here are within the uncertainties of this estimate (e.g. Riley et al., 2013). The same termite emissions are used in all simula-

BGD

12, 2161–2212, 2015

Seasonal and inter-annual variability in wetland methane emissions

L. Meng et al.

Title Page

Abstract

Introduction

Conclusions

References

Tables

Figures



Back

Close

Full Screen / Esc

Printer-friendly Version

Interactive Discussion



tions. The global interannual average of methane emissions used in CN_a, CN_b and BGC are similar to that used in TransCom.

2.2 CLM4Me'

CLM4Me' (Meng et al., 2012) is a process-based methane biogeochemical models incorporated in the CLM version 4 and CLM version 4.5 of the Community Earth System Model (CESM). CLM4Me' is based on CLM4Me (Riley et al., 2011) and explicitly calculates methane production, methane oxidation, methane ebullition, methane diffusion through soils, and methane transport through aerenchyma. CLM4Me' is an update of CLM4Me to include a pH and redox functional dependence for methane emissions, and a limitation of aerenchyma in plants in always-inundated areas (Meng et al., 2012). A detailed description of CLM4Me and CLM4Me' can be found in Meng et al. (2012) and Riley et al. (2011). In this study, CLM4Me' is forced with multi-satellite derived inundation fraction (Prigent et al., 2007) and NCEP (i.e., the National Center for Environmental Prediction) reanalysis datasets (Kistler et al., 2001; Qian et al., 2006). Model spin-up is described in Meng et al. (2012). While the simulation period is 1990–2005 satellite inundation data is only available from 1993–2004. We use climatological monthly average (1993–2004) inundation fraction for years 1990–1992 and 2005.

2.3 Community land model (CLM)

The CLM4Me' is integrated and spun up in two versions of the CLM: CLM4.0 and CLM4.5. The CLM4.0 uses the carbon and nitrogen below ground module from the Carbon-Nitrogen (CN) model (Thornton et al., 2007, 2009). The CLM4.5 is updated from the CLM4.0 and offers some improvements with the most significant change to the below ground carbon cycle (Koven et al., 2013). The CLM4.5 includes an alternate decomposition cascade from the Century soil model, which is referred to as the biogeochemistry version of the model (CLM4.5-BGC). This version of the model has increased productivity and carbon in high latitudes (perhaps an overestimate) and re-

BGD

12, 2161–2212, 2015

Seasonal and inter-annual variability in wetland methane emissions

L. Meng et al.

Title Page

Abstract

Introduction

Conclusions

References

Tables

Figures

◀

▶

◀

▶

Back

Close

Full Screen / Esc

Printer-friendly Version

Interactive Discussion



tions. In addition a soil sink for CH₄ is included using a climatological monthly average derived from LMDZ atmospheric CH₄ inversion (Bousquet et al., 2006).

Atmospheric concentrations of methane are tagged from the rice paddy, wetland, anthropogenic and biomass burning emission sources. The losses of tagged methane are identical to those described above.

2.5 Observed atmospheric CH₄ concentration

Observational atmospheric CH₄ concentration datasets are obtained from the World Data Centre for Greenhouse Gases (WDCGG) at <http://ds.data.jma.go.jp/gmd/wdcgg/>. Monthly concentration datasets from 14 stations (Table 2) around the world are compared with the simulated atmospheric CH₄ (Butler et al., 2004; Cunnold et al., 2002). Most of the sites have monthly or weekly measurements and use flask-sampling method. Collected samples are analyzed using gas chromatography with flame ionization detection (Dlugokencky et al., 2005).

2.6 RMS variability

Seasonal and inter-annual Root Mean Square (RMS) variability are used to evaluate the spatial distribution of simulated methane variability. We apply the method described in Nevison et al. (2008). Here, seasonal RMS variability is calculated as the RMS of the differences between model climatological monthly means (1990–2004) and the climatological annual mean. The interannual variability of RMS is calculated as the RMS of the differences between each month and the corresponding month from the climatological seasonal cycle. We calculate RMS separately for methane tagged from each tagged emission source. This apportions the variability of each source by calculating the ratio between the variability due to that source RMS and the total RMS. Please note that the sum of individual source's contribution to total RMS is often greater than 1 in cases of cancelation of signals among individual sources.

BGD

12, 2161–2212, 2015

Seasonal and inter-annual variability in wetland methane emissions

L. Meng et al.

Title Page

Abstract

Introduction

Conclusions

References

Tables

Figures

◀

▶

◀

▶

Back

Close

Full Screen / Esc

Printer-friendly Version

Interactive Discussion



sions used in CN_a and CN_b experiments are slightly higher (lower) than that used in TransCom experiment during the first (second) half of the study period (Fig. 4). The annual total emissions used in BGC are slightly lower than those used in TransCom during most years except 1997, 1998, and 2002. There are no statistically significant trends (at $\sim 95\%$ level) in the difference between the BGC and TransCom total emissions.

3.2 Seasonal and inter-annual variability in CN_a and BGC methane emissions

3.2.1 CN_a methane emissions

There are strong seasonal and inter-annual variations in CN_a wetland methane emissions (Fig. 5). On a seasonal basis, the peak methane emissions occur in the summer and the lowest methane emissions occur in winter as methane emission is controlled by both temperatures and inundated area. On an inter-annual basis, the summer of 1994 has the highest methane fluxes in the period of 1993–2004 in CN_a methane emissions. A generally decreasing trend ($-2.1 \text{ Tg CH}_4 \text{ yr}^{-1}$, significant at 95% level) in CN_a global wetland emissions occur from 1994 to 2004 driven by trends in tropical wetland emissions (Fig. 5) as tropical wetlands contribute to $\sim 78\%$ of the global wetland flux. The decreasing rate in tropical wetland emissions from 1993–2004 is approximately $-1.68 \text{ Tg CH}_4 \text{ yr}^{-1}$, statistically significantly different from 0 (no change) at the 95% confidence level.

We further identify the four highest (1994, 1995, 1996, 1999) and lowest (2001, 2002, 2003, 2004) annual CN_a methane emissions in the period of 1993–2004 and plot the difference in spatial distribution of methane emissions between the average of the 4 extreme high and low emission years (Fig. 6a). There are large increases across much of the globe, but the largest difference occurs in the tropics (see the latitudinal average on the left). This is not surprising given the tropical regions contribute to approximately 78% of the global wetland flux in this model configuration. At regional level, the largest

BGD

12, 2161–2212, 2015

Seasonal and inter-annual variability in wetland methane emissions

L. Meng et al.

Title Page

Abstract

Introduction

Conclusions

References

Tables

Figures

⏪

⏩

◀

▶

Back

Close

Full Screen / Esc

Printer-friendly Version

Interactive Discussion



differences are primarily present in Indonesia and South America (e.g., Amazon regions).

3.2.2 BGC methane emissions

The trend in BGC wetland methane emissions is different from that in CN_a experiment (Fig. 5). In the BGC simulation, the peak emissions occur in 2002 instead of 1994. The wetland emissions do not decrease significantly from 1993 to 2004 with no significant trends in the inter-annual methane emissions in the mid- and high- latitudes and the tropics in these simulations. There are several additional differences between CN_a and BGC wetland emissions: (1) BGC wetland emissions are approximately 10% lower than CN_a wetland emissions; (2) BGC estimates the tropical (-30°S – 20°N) wetland emissions to be $63\text{ Tg CH}_4\text{ yr}^{-1}$, approximately 60% lower than those in CN_a ($158\text{ Tg CH}_4\text{ yr}^{-1}$); (3) high latitudes ($>50^{\circ}\text{N}$) wetland emissions in BGC are $97\text{ Tg CH}_4\text{ yr}^{-1}$ while CN_a only produces $12\text{ Tg CH}_4\text{ yr}^{-1}$. Such large differences are probably largely due to the shift of carbon from tropics to high latitudes as a result of the modifications from CN_a to BGC (i.e., the multi-level biogeochemistry) (Koven et al., 2013). BGC and CN_a produce similar methane emissions in the mid-latitudes (20 – 50°N).

The latitudinal distribution of the methane emissions in CN_a suggests the largest seasonal variation occurs at approximately 20 – 30°N , followed by the latitudinal band 50 – 60°N (Fig. 7a). High latitudes ($>65^{\circ}\text{N}$) have no clear seasonal cycles due to the low methane fluxes that CN_a produces in the high latitudes (Meng et al., 2012). There is a very dampened seasonal variation of CH_4 emissions in tropical wetlands (10°S – 10°N), although tropical wetlands are the largest contribution to total wetland emissions. The seasonal cycle shown in Fig. 7a in different latitudinal bands is consistent with that identified in Spahni et al. (2011) (see their Fig. 4a).

The latitudinal distribution of methane emissions shows a strong seasonal variation in high latitudes in BGC. As clearly shown in Fig. 7b, peak methane emis-

BGD

12, 2161–2212, 2015

Seasonal and inter-annual variability in wetland methane emissions

L. Meng et al.

Title Page

Abstract

Introduction

Conclusions

References

Tables

Figures

◀

▶

◀

▶

Back

Close

Full Screen / Esc

Printer-friendly Version

Interactive Discussion



sions ($> 200 \text{ mg CH}_4 \text{ m}^{-2} \text{ day}^{-1}$) occur in summer seasons and low methane emissions ($\sim 10 \text{ mg CH}_4 \text{ m}^{-2} \text{ day}^{-1}$) are present in winter. The maximum emissions occur at approximately 60° N as distinct from the CN_a simulations.

The peak emissions in BGC from 1993–2004 occur in 1998 followed by 2002, 1994, and 2003. The four lowest emission years are 1999, 2000, 2001, and 1996. As shown in Fig. 6b, the increase in methane emissions between the four lowest to highest years is primarily on the equator, in the Southern Hemisphere (around 30° S) and in the high latitudes ($50\text{--}70^\circ \text{ N}$). This is distinct from the CN_a simulations where the largest change predominantly occurs in the tropics (Fig. 6a).

3.3 Contribution of individual sources to seasonal and inter-annual variability in atmospheric CH_4

In order to determine the relative contribution of each source to total atmospheric CH_4 variability as simulated in CAM-chem model, we calculate the seasonal and inter-annual Root Mean Square (RMS) variability for the total CH_4 concentration and the partial contribution of the anthropogenic source, rice paddies, and wetlands to the overall RMS (Figs. 8 and 9). These three sources have the largest contribution to the annual RMS due to their large magnitudes.

3.3.1 Seasonal and inter-annual variability in CN_a methane emissions

Seasonal variability of atmospheric methane concentration is high in the tropics and Southern Hemisphere and low in the northern high latitudes. The low seasonal variability in the northern high latitudes is consistent with the relatively low magnitude of northern high latitude methane fluxes, plus the fact that the highest emissions occur during the summer, when the vertical mixing is highest.

Inter-annual variability (IAV) in RMS is relatively homogeneous across the globe with slightly higher IAV in the Southern Hemisphere. IAV RMS of atmospheric methane is generally larger than the seasonal RMS. Both anthropogenic sources and wetlands are

BGD

12, 2161–2212, 2015

Seasonal and inter-annual variability in wetland methane emissions

L. Meng et al.

Title Page

Abstract

Introduction

Conclusions

References

Tables

Figures

⏪

⏩

◀

▶

Back

Close

Full Screen / Esc

Printer-friendly Version

Interactive Discussion



the dominant contributors to the seasonal RMS variability in the Northern Hemisphere (Fig. 8), while wetlands are the only dominant contributor to the IAV RMS variability. This is in agreement with Bousquet et al. (2006) that wetland emissions dominate the inter-annual variability of methane sources. Rice paddies play a more important role in seasonal RMS variability than in inter-annual RMS variability over Asia and North America. This is consistent with the largest seasonal variations in rice paddy emissions occur over Asia and North America (Meng et al., 2013). Similar results are also found in CN_b simulations.

3.3.2 Seasonal and inter-annual variability in BGC methane emissions

Compared to CN_a, the BGC methane emissions show higher seasonal and inter-annual variability, particularly in high-latitudes (Fig. 9). For instance, Alaska and Siberia are two regions that have the highest variability. For both the seasonal and inter-annual variations, wetlands dominate the variability, followed by anthropogenic sources. Rice paddies only play a role in the tropics (0–30° N). Both wetlands and anthropogenic methane emissions in BGC contribute a higher percentage to the inter-annual variations than in CN_a simulations.

3.4 Interhemispheric gradients in atmospheric CH₄ concentrations

The latitudinal gradient from TransCom, CN_a, CN_b, BGC, and observations is shown in Fig. 10. The latitudinal gradient is defined as the difference in averaged CH₄ concentration between Northern and Southern Hemispheres (N–S gradients) stations listed in Table 2. The N–S gradients produced in all four simulations are highly correlated with observations for the period of 1993–2004 (Fig. 10). The correlations (r) are 0.83, 0.72, 0.76, 0.91 for TransCom, CN_a, CN_b, and BGC, respectively. It is also clearly shown in Fig. 10 that the TransCom and CN_a simulations underestimate the N–S Hemisphere gradients. The underestimation of N–S gradients in CN_a might be due to the high tropical wetland emissions in this case as the high tropical emissions are likely to

BGD

12, 2161–2212, 2015

Seasonal and inter-annual variability in wetland methane emissions

L. Meng et al.

Title Page

Abstract

Introduction

Conclusions

References

Tables

Figures

⏪

⏩

◀

▶

Back

Close

Full Screen / Esc

Printer-friendly Version

Interactive Discussion



overpredict the amplitude of the inter-annual variability. Decreasing wetland emissions (CN_b) allows for a better match between model simulations and observations. This suggests that CN_a simulations might overestimate wetland emissions, which agrees with the findings in Kirschke et al. (2013).

3.6 Methane growth rate

The growth rate refers to the average increase in atmospheric CH₄ concentration per year. We calculate the growth rate at each station from the observations and for each simulation. The observed average growth rate ranges from 3.2 to 4.6 ppb yr⁻¹ with an average of 4.0 ppb yr⁻¹ (Fig. 14, Table 3). The average growth rate in TransCom, CN_a, CN_b, and BGC experiments is 4.2, 3.29, 4.05, and 5.68 ppb yr⁻¹, respectively (Table 3). The growth rate in TransCom, CN_a, CN_b and BGC simulations has a large range (from -0.48 to 6.44 ppb yr⁻¹) at all stations analyzed. As can be seen from Fig. 14, both CN_a and CN_b tend to underestimate the observed growth rate in Northern Hemisphere, but overestimate it in Southern Hemisphere (Fig. 14) except for the South Pole station. BGC tends to overestimate growth rate in the Northern Hemisphere, particularly in the high latitudes (Fig. 14). TransCom gives better agreement with the measured growth rates in the Southern Hemisphere than in the Northern Hemisphere. The largest difference in the growth rate between the three cases and the observations occur at the Zeppelinfjellet (zep, Norway) where the average growth rate in TransCom, CN_a, CN_b, BGC and observations was -0.92, -0.48, 1.99, 4.2, and 3.4 ppb yr⁻¹, respectively (Table 3). The largest difference between BGC and observations is at Barrow, where the growth rate in BGC experiment was approximately 2 times of that in observations. Overall, CN_a and CN_b underestimate the station growth rate in high latitudes while BGC overestimates it.

In addition, a summary of the comparison of model N-S gradients, annual growth rates, and inter-annual variability with observations is presented in Fig. 15. Four stations are specifically selected to represent the South Pole, tropical region, mid-latitudes, and high northern latitudes. Root mean square errors and biases for the four simula-

Seasonal and inter-annual variability in wetland methane emissions

L. Meng et al.

Title Page

Abstract

Introduction

Conclusions

References

Tables

Figures



Back

Close

Full Screen / Esc

Printer-friendly Version

Interactive Discussion



tions at these four stations are listed in Table 4. As seen in Fig. 15, and discussed above, no one model simulation best matches all the observational metrics.

3.7 Comparison of inter-annual variability between this study and others

We also compare the inter-annual variability in CH₄ emission anomalies in the simulations analyzed here with those given in Spahni et al. (2011), in an updated long term atmospheric synthesis inversion from Bousquet et al. (2006) and from Ringeval et al. (2010) (Fig. 16). As discussed above, the CN_a emissions reach their maximum in 1994 and decrease thereafter from 1994–2004 (Fig. 16). The BGC emissions have the highest emissions in 1998 followed by the lowest emissions in 1999 and increased from 1999 to 2004. The TransCom emissions increase from 1993 to 1998 and slightly decrease since then. The wetland emissions in Ringeval et al. (2010) decrease from 1993–2000. The Ringeval et al. (2010) averaged annual wetland methane emissions are $\sim 215 \text{ Tg yr}^{-1}$, similar to the CN_a wetland emissions. However, the atmospheric synthesis inversions of global wetlands (update of Bousquet et al., 2006, constant OH) wetland emissions increase from 1990 to 2000 followed by a decrease from 2000 to 2005.

We further compare our model-derived wetland emissions with those from Wetland Model Inter-comparison of Models Project (WETCHIMP) (Melton et al., 2013; Wania et al., 2013). We conduct two different comparisons: one comparison includes all models with their different wetland determination schemes while the other focuses on models that are driven by satellite inundation datasets (see Table 1, Melton et al., 2013).

Each model analyzed in Melton et al. (2013) uses a different wetland parameterization to estimate their wetland extent (see Table 1 in Melton et al., 2013 for details). Therefore, it is not surprising to see the large variation in the wetland extent among all these models from 1993–2004 (Fig. 17). Amongst the models analyzed in Melton et al. (2013) only the LPJ-WSL model uses a prescribed monthly inundation datasets, similar to our simulations (Fig. 17). DLEM_{norice} prescribes maximum extents at each gridcell from satellite inundation datasets but with simulated intra-annual dynamics. All

Seasonal and inter-annual variability in wetland methane emissions

L. Meng et al.

Title Page

Abstract

Introduction

Conclusions

References

Tables

Figures



Back

Close

Full Screen / Esc

Printer-friendly Version

Interactive Discussion



the simulations making use of the satellite measurements (this study, LPJ-WSL, BGC, and DLEM_norice) show a decrease in wetland extents from 1993–2004. The wetland extent anomalies in DLEM_norice simulations differ as the intra-annual dynamics are simulated (Fig. 17).

The models that do not use a prescribed satellite inundation dataset do not simulate notable decreases in wetland extents during the period of 1993–2004. This is not in agreement with the satellite inundation dataset: Papa et al. (2010) find ~5.7% decrease in mean annual maximum inundation from 1993 to 2004 with maximum decrease in the tropics. In fact, all models (excluding LPJ-WSL, DLEM_norice, and this study) show large increases in wetland extents in 1998 compared to that in 1997, which is also documented in Melton et al. (2013).

Melton et al. (2013) demonstrate that the difference in wetland area used in different models might partially explain the discrepancy in model estimated wetland emissions. As shown in Melton et al. (2013), model-derived methane emissions are strongly correlated with the wetland extent (with an average correlation of 0.90 on the global scale). All models that produce a peak methane emission in 1998 have a maximum wetland extent at the same time (Fig. 18). The difference in model-derived methane emission can be attributed partially to the different wetland area used in each model, where the wetland extent is highly uncertain (Melton et al., 2013). However, it should be noted that there are several limitations associated with using wetland extents derived from satellite inundation datasets. As suggested in Prigent et al. (2007), satellites might underestimate inundated areas due to their incapability to detect small water bodies. Further, satellite datasets only include fully inundated area and excluded unsaturated wet mineral soils, which might also be important wetland methane source (Spahni et al., 2011).

The methane emission anomalies in DLEM_norice and LPJ_WSL (the simulations in Melton et al. (2013) using satellite or satellite derived wetland extent) show similar temporal variations, as do the methane anomalies in CN_a and CN_b simulations (Fig. 19). Emissions estimated in CN_a, CN_b, DLEM_norice, and LPJ_WSL peak in

BGD

12, 2161–2212, 2015

Seasonal and inter-annual variability in wetland methane emissions

L. Meng et al.

Title Page

Abstract

Introduction

Conclusions

References

Tables

Figures



Back

Close

Full Screen / Esc

Printer-friendly Version

Interactive Discussion



1993–1994 and decrease since then. Such a decreasing trend is consistent with the decrease in wetland extents used in these models (Fig. 17). The CN_a and CN_b simulations show a large increase in emissions from 1993 to 1994, but do not simulate large increases in methane emissions from 2001 to 2002 even though wetland extents increase during this period. It should be noted that the BGC simulation uses the same wetland extent as CN_a and CN_b but does not give the same large decrease in the emissions during the period of 1993–2004. In fact, the BGC model gives decreasing emissions from 1993–1994 but increasing methane emissions from 2001–2002. The BGC model also shows that the highest emission occurs in 1998 and the lowest in 1999 during the period of 1993–2004.

Both the large increase in the methane emissions from 1993 to 1994 in CN_a and CN_b and the small increase from 2001 to 2002 are likely due to the changes in heterotrophic respiration (HR) in CN_a simulations (Fig. 20). HR increases dramatically in CN_a from 1993 to 1994 (Fig. 20) driving higher methane emissions whereas the decrease in HR from 2001 to 2002 decreases wetland methane production, which might offset the increase in methane emissions from wetland extents. The HR in the BGC simulation is rather different, consistent with the different behavior between CN_a and CN_b and the BGC simulations. Zhao et al. (2005) estimate the net primary production (NPP) from satellites and found that NPP in 2001 is higher than those in 2002 and 2003. Please note that NPP is closely related to HR. The correlation of global wetland emissions with HR and wetland extents is 0.81 and 0.94, respectively, in CN_a simulations. In BGC simulations, simulated global wetland emissions are also highly correlated with HR (0.89) and with wetland extents (0.81), respectively. Such high correlations suggest that both HR and wetland extents are dominate drivers of wetland methane emissions in CN_a and BGC models. Thus, although BGC experiment uses the same satellite inundated area in CN_a, it does not produce a decreasing trend in methane emissions during the period, probably due to its different trend in HR estimated in BGC as compared with that in CN_a (Fig. 20).

Seasonal and inter-annual variability in wetland methane emissions

L. Meng et al.

[Title Page](#)[Abstract](#)[Introduction](#)[Conclusions](#)[References](#)[Tables](#)[Figures](#)[⏪](#)[⏩](#)[◀](#)[▶](#)[Back](#)[Close](#)[Full Screen / Esc](#)[Printer-friendly Version](#)[Interactive Discussion](#)

4 Conclusions

In this study, we evaluate the temporal and spatial patterns in wetland methane emissions simulated in the CLM4Me' from both CLM4.0 (CN_a and CN_b) and CLM4.5 (BGC). We show strong seasonal and inter-annual variations in wetland methane emissions. In both CN_a and BGC the largest methane emissions occur in the Northern Hemisphere summer. There are several large differences in the inter-annual and spatial variations in CN_a and BGC wetland emissions. On an inter-annual basis during the period of 1993–2004, methane emissions simulated in CN_a peak in 1994 and decrease thereafter. Such a decrease is consistent with a decreasing tropical inundated area, based on observations (Papa et al., 2010; Prigent et al., 2007). Since CN_a experiment has very strong tropical emissions, changes in the tropics dominated the global emissions.

On the other hand, CLM4Me' methane emissions driven by CLM4.5 (the BGC simulation) are highest in 1999 and do not show the significant decrease during the period 1993–2004. Compared to CN_a simulations, BGC produces large emissions in the high latitudes with very strong seasonal variations and relatively small wetland emissions in the tropical region. The spatial distribution of emission differences between the four highest and lowest emissions years in the BGC simulation show the large differences in the high latitudes, tropics, and Southern Hemisphere (around 30° S) in BGC (Koven et al., 2013).

The comparison of the IAV demonstrates large disagreements between different estimates of the annual wetland emissions. CN_a wetland emissions suggest a decreasing trend from 1994 to 2004, which is similar to those estimates from Ringer et al. (2010) and DLEM_norice and LPJ-WSL models (Melton et al., 2013; Wania et al., 2013). The updated estimate from Bousquet et al. (2006) gives increasing emissions from 1991–2000 and a decrease after 2000. A few participating wetland emission models in the WETCHIM project also predict a peak methane emission in the middle of the period (around 1998–1999). For instance, all models (excluding DLEM_norice and LPJ-WSL)

BGD

12, 2161–2212, 2015

Seasonal and inter-annual variability in wetland methane emissions

L. Meng et al.

Title Page

Abstract

Introduction

Conclusions

References

Tables

Figures



Back

Close

Full Screen / Esc

Printer-friendly Version

Interactive Discussion



BGD

12, 2161–2212, 2015

Seasonal and
inter-annual
variability in wetland
methane emissions

L. Meng et al.

Title Page

Abstract

Introduction

Conclusions

References

Tables

Figures

◀

▶

◀

▶

Back

Close

Full Screen / Esc

Printer-friendly Version

Interactive Discussion



observations than CN_a and CN_b simulations. In the TransCom experiment, the magnitude of the correlation between modeled atmospheric concentrations and observations is similar to that of the BGC experiment. We also find that CN_b experiments tend to underestimate the growth rate and BGC overestimates it in high latitudes. TransCom simulations have an overall better estimation of the growth rate at all stations than the other three simulations. In terms of the N–S gradients, CN_b experiments have the closest match with observations among all experiments. BGC overestimated the N–S gradients by $\sim 70\%$ while CN_a and TransCom underestimate it by $\sim 10\%$ and $\sim 20\%$, respectively. Please note that BGC uses much higher methane emissions from the high latitudes ($> 50^\circ \text{N}$) than CN_a and CN_b experiments. These simulations generally suggest that the high latitude methane emissions should be somewhere in the broad range between those used in CN_b ($\sim 7.7 \text{ Tg yr}^{-1}$) and BGC ($\sim 97 \text{ Tg yr}^{-1}$). This study confirms that the large variation in methane emissions exist and they play an important role in affecting atmospheric methane concentration (Bousquet et al., 2006).

In CN_a simulations, tropical wetlands contribute to approximately 78 % of the global wetland fluxes and high latitudes ($> 50^\circ \text{N}$) only release less than 10 % of the global wetland fluxes. While in BGC, high latitude wetlands contribute more to the global wetland fluxes than the tropical wetlands. Both CN_a and BGC methane simulations are forced with the same satellite inundated fraction, they produce large differences in both spatial and temporal variations of methane emissions due to the fact that CN_a and BGC use different carbon cycle models. This suggests that model estimated methane budget is sensitive not only to wetland extents, but also to the carbon pool where the methane is produced (Melton et al., 2013). Further research might need to focus on regional wetlands (such as high-latitude and tropical wetlands) in order to have a better estimate of wetland methane budget and its spatial variation.

Acknowledgements. The authors would like to thank Joe Melton for providing model datasets from the Wetland and Wetland CH_4 Inter-comparison of Models Project (WETCHIMP). Part of the work was supported by NASA grant DE-SC0006791.

References

- Bloom, A. A., Palmer, P. I., Fraser, A., Reay, D. S., and Frankenberg, C.: Large-Scale Controls of Methanogenesis Inferred from Methane and Gravity Spaceborne Data, *Science*, 327, 322–325, 2010.
- 5 Bloom, A. A., Palmer, P. I., Fraser, A., and Reay, D. S.: Seasonal variability of tropical wetland CH₄ emissions: the role of the methanogen-available carbon pool, *Biogeosciences*, 9, 2821–2830, doi:10.5194/bg-9-2821-2012, 2012.
- Bousquet, P., Ciais, P., Miller, J. B., Dlugokencky, E. J., Hauglustaine, D. A., Prigent, C., Van der Werf, G. R., Peylin, P., Brunke, E. G., Carouge, C., Langenfelds, R. L., Lathiere, J.,
10 Papa, F., Ramonet, M., Schmidt, M., Steele, L. P., Tyler, S. C., and White, J.: Contribution of anthropogenic and natural sources to atmospheric methane variability, *Nature*, 443, 439–443, doi:10.1038/Nature05132, 2006.
- Butler, J. H., Daube, B. C., Dutton, G. S., Elkins, J. W., Hall, B. D., Hurst, D. F., King, D. B., Kling, E. S., Laflour, B. G., Lind, J., Lovitz, S., Mondeel, D. J., Montzka, S. A., Moore, F. L.,
15 Nance, J. D., Neu, J. L., Romashkin, P. R., Sheffer, A., and Snible, W. J.: Halocarbons and other atmospheric trace species, NOAA/US Department of Commerce, Boulder, Colorado, 2004.
- Cunnold, D. M., Steele, L. P., Fraser, P. J., Simmonds, P. G., Prinn, R. G., Weiss, R. F., Porter, L. W., O'Doherty, S., Langenfelds, R. L., Krummel, P. B., Wang, H. J., Emmons, L., Tie, X. X., and Dlugokencky, E. J.: In situ measurements of atmospheric methane at GAGE/AGAGE
20 sites during 1985–2000 and resulting source inferences, *J. Geophys. Res.-Atmos.*, 107, ACH 20-1–ACH 20-18, doi:10.1029/2001JD001226, 2002.
- Denman, K. L., Brasseur, G., Chidthaisong, A., Ciais, P., Cox, P. M., Dickinson, R. E., Hauglustaine, D., Heinze, C., Holland, E., Jacob, D., Lohmann, U., Ramachandran, S., da Silva Dias, P. L., Wofsy, S. C., and Zhang, X.: Couplings Between Changes in the Climate System and Biogeochemistry, in: *Climate Change 2007: The Physical Science Basis. Contribution of Working Group I to the Fourth Assessment Report of the Intergovernmental Panel on Climate Change*, edited by: Solomon, S., Qin, D., Manning, M., Chen, Z., Marquis, M., Averyt, K. B., Tignor, M., and Miller, H. L., Cambridge University Press, Cambridge, United Kingdom
25 and New York, NY, USA, 2007.
- Dlugokencky, E. J., Myers, R. C., Lang, P. M., Masarie, K. A., Crotwell, A. M., Thoning, K. W., Hall, B. D., Elkins, J. W., and Steele, L. P.: Conversion of NOAA atmospheric dry air CH₄

BGD

12, 2161–2212, 2015

Seasonal and inter-annual variability in wetland methane emissions

L. Meng et al.

Title Page

Abstract

Introduction

Conclusions

References

Tables

Figures

◀

▶

◀

▶

Back

Close

Full Screen / Esc

Printer-friendly Version

Interactive Discussion



Seasonal and inter-annual variability in wetland methane emissions

L. Meng et al.

Title Page

Abstract

Introduction

Conclusions

References

Tables

Figures



Back

Close

Full Screen / Esc

Printer-friendly Version

Interactive Discussion



Koven, C. D., Riley, W. J., Subin, Z. M., Tang, J. Y., Torn, M. S., Collins, W. D., Bonan, G. B., Lawrence, D. M., and Swenson, S. C.: The effect of vertically resolved soil biogeochemistry and alternate soil C and N models on C dynamics of CLM4, *Biogeosciences*, 10, 7109–7131, doi:10.5194/bg-10-7109-2013, 2013.

5 Lamarque, J.-F., Emmons, L. K., Hess, P. G., Kinnison, D. E., Tilmes, S., Vitt, F., Heald, C. L., Holland, E. A., Lauritzen, P. H., Neu, J., Orlando, J. J., Rasch, P. J., and Tyndall, G. K.: CAM-chem: description and evaluation of interactive atmospheric chemistry in the Community Earth System Model, *Geosci. Model Dev.*, 5, 369–411, doi:10.5194/gmd-5-369-2012, 2012.

10 Melton, J. R., Wania, R., Hodson, E. L., Poulter, B., Ringeval, B., Spahni, R., Bohn, T., Avis, C. A., Beerling, D. J., Chen, G., Eliseev, A. V., Denisov, S. N., Hopcroft, P. O., Lettenmaier, D. P., Riley, W. J., Singarayer, J. S., Subin, Z. M., Tian, H., Zürcher, S., Brovkin, V., van Bodegom, P. M., Kleinen, T., Yu, Z. C., and Kaplan, J. O.: Present state of global wetland extent and wetland methane modelling: conclusions from a model inter-comparison project (WETCHIMP), *Biogeosciences*, 10, 753–788, doi:10.5194/bg-10-753-2013, 2013.

15 Meng, L., Hess, P. G. M., Mahowald, N. M., Yavitt, J. B., Riley, W. J., Subin, Z. M., Lawrence, D. M., Swenson, S. C., Jauhiainen, J., and Fuka, D. R.: Sensitivity of wetland methane emissions to model assumptions: application and model testing against site observations, *Biogeosciences*, 9, 2793–2819, doi:10.5194/bg-9-2793-2012, 2012.

20 Mitchell, T. D. and Jones, P. D.: An improved method of constructing a database of monthly climate observations and associated high-resolution grids, *Int. J. Climatol.*, 25, 693–712, 2005.

Montzka, S. A., Krol, M., Dlugokencky, E., Hall, B., Jockel, P., and Lelieveld, J.: Small Interannual Variability of Global Atmospheric Hydroxyl, *Science*, 331, 67–69, 2011.

25 Olivier, J. G. J. and Berdowski, J. J. M.: Global emissions sources and sinks, *The Climate System*, edited by: Berdowski, J., Guicherit, R., and Heij, B. J., Swets & Zeitlinger Pub., Lisse, the Netherlands, 2001.

Papa, F., Prigent, C., Aires, F., Jimenez, C., Rossow, W. B., and Matthews, E.: Interannual variability of surface water extent at the global scale, 1993–2004, *J. Geophys. Res.-Atmos.*, 115, D12111, doi:10.1029/2009JD012674, 2010.

30 Patra, P. K., Houweling, S., Krol, M., Bousquet, P., Belikov, D., Bergmann, D., Bian, H., Cameron-Smith, P., Chipperfield, M. P., Corbin, K., Fortems-Cheiney, A., Fraser, A., Gloor, E., Hess, P., Ito, A., Kawa, S. R., Law, R. M., Loh, Z., Maksyutov, S., Meng, L., Palmer, P. I., Prinn, R. G., Rigby, M., Saito, R., and Wilson, C.: TransCom model simulations of

Seasonal and inter-annual variability in wetland methane emissions

L. Meng et al.

[Title Page](#)

[Abstract](#)

[Introduction](#)

[Conclusions](#)

[References](#)

[Tables](#)

[Figures](#)



[Back](#)

[Close](#)

[Full Screen / Esc](#)

[Printer-friendly Version](#)

[Interactive Discussion](#)



CH₄ and related species: linking transport, surface flux and chemical loss with CH₄ variability in the troposphere and lower stratosphere, *Atmos. Chem. Phys.*, 11, 12813–12837, doi:10.5194/acp-11-12813-2011, 2011.

Popova, Z. and Kercheva, M.: CERES model application for increasing preparedness to climate variability in agricultural planning – calibration and validation test, *Phys. Chem. Earth*, 30, 125–133, 2005.

Prigent, C., Papa, F., Aires, F., Rossow, W. B. and Matthews, E.: Global inundation dynamics inferred from multiple satellite observations, 1993–2000, *J. Geophys. Res.-Atmos.*, 112, D12107, doi:10.1029/2006JD007847, 2007.

Qian, T. T., Dai, A., Trenberth, K. E., and Oleson, K. W.: Simulation of global land surface conditions from 1948 to 2004. Part I: Forcing data and evaluations, *J. Hydrometeorol.*, 7, 953–975, 2006.

Rigby, M., Prinn, R. G., Fraser, P. J., Simmonds, P. G., Langenfelds, R. L., Huang, J., Cunnold, D. M., Steele, L. P., Krummel, P. B., Weiss, R. F., O'Doherty, S., Salameh, P. K., Wang, H. J., Harth, C. M., Mühle, J., and Porter, L. W.: Renewed growth of atmospheric methane, *Geophys. Res. Lett.*, 35, L22805, doi:10.1029/2008GL036037, 2008.

Riley, W. J., Subin, Z. M., Lawrence, D. M., Swenson, S. C., Torn, M. S., Meng, L., Mahowald, N. M., and Hess, P.: Barriers to predicting changes in global terrestrial methane fluxes: analyses using CLM4Me, a methane biogeochemistry model integrated in CESM, *Biogeosciences*, 8, 1925–1953, doi:10.5194/bg-8-1925-2011, 2011.

Shannon, R. D. and White, J. R.: 3-Year Study of Controls on Methane Emissions from 2 Michigan Peatlands, *Biogeochemistry*, 27, 35–60, 1994.

Simmons, A. J. and Gibson, J. K.: The ERA-40 Project Plan, ERA-40 Project Report Series 1, 63 pp., 2000.

Spahni, R., Wania, R., Neef, L., van Weele, M., Pison, I., Bousquet, P., Frankenberg, C., Foster, P. N., Joos, F., Prentice, I. C., and van Velthoven, P.: Constraining global methane emissions and uptake by ecosystems, *Biogeosciences*, 8, 1643–1665, doi:10.5194/bg-8-1643-2011, 2011.

Taylor, K. E.: Summarizing multiple aspects of model performance in a single diagram, *J. Geophys. Res.-Atmos.*, 106, 7183–7192, 2001.

Thornton, P. E., Lamarque, J. F., Rosenbloom, N. A., and Mahowald, N. M.: Influence of carbon-nitrogen cycle coupling on land model response to CO₂ fertilization and climate variability, *Global Biogeochem. Cy.*, 21, Gb4018, doi:10.1029/2006gb002868, 2007.

Seasonal and inter-annual variability in wetland methane emissions

L. Meng et al.

Title Page

Abstract

Introduction

Conclusions

References

Tables

Figures

◀

▶

◀

▶

Back

Close

Full Screen / Esc

Printer-friendly Version

Interactive Discussion



Thornton, P. E., Doney, S. C., Lindsay, K., Moore, J. K., Mahowald, N., Randerson, J. T., Fung, I., Lamarque, J.-F., Feddesma, J. J., and Lee, Y.-H.: Carbon-nitrogen interactions regulate climate-carbon cycle feedbacks: results from an atmosphere-ocean general circulation model, *Biogeosciences*, 6, 2099–2120, doi:10.5194/bg-6-2099-2009, 2009.

5 van der Werf, G. R., Randerson, J. T., Giglio, L., Collatz, G. J., Kasibhatla, P. S., and Arellano Jr., A. F.: Interannual variability in global biomass burning emissions from 1997 to 2004, *Atmos. Chem. Phys.*, 6, 3423–3441, doi:10.5194/acp-6-3423-2006, 2006.

Wania, R., Melton, J. R., Hodson, E. L., Poulter, B., Ringeval, B., Spahni, R., Bohn, T., Avis, C. A., Chen, G., Eliseev, A. V., Hopcroft, P. O., Riley, W. J., Subin, Z. M., Tian, H., van Bodegom, P. M., Kleinen, T., Yu, Z. C., Singarayer, J. S., Zürcher, S., Lettenmaier, D. P., Beerling, D. J., Denisov, S. N., Prigent, C., Papa, F., and Kaplan, J. O.: Present state of global wetland extent and wetland methane modelling: methodology of a model inter-comparison project (WETCHIMP), *Geosci. Model Dev.*, 6, 617–641, doi:10.5194/gmd-6-617-2013, 2013.

10 Wuebbles, D. J. and Hayhoe, K.: Atmospheric methane and global change., *Earth-Sci. Rev.*, 57, 177–210, 2002.

15 Xu, X. F., Tian, H. Q., Zhang, C., Liu, M. L., Ren, W., Chen, G. S., Lu, C. Q., and Bruhwiler, L.: Attribution of spatial and temporal variations in terrestrial methane flux over North America, *Biogeosciences*, 7, 3637–3655, doi:10.5194/bg-7-3637-2010, 2010.

Seasonal and inter-annual variability in wetland methane emissions

L. Meng et al.

[Title Page](#)

[Abstract](#)

[Introduction](#)

[Conclusions](#)

[References](#)

[Tables](#)

[Figures](#)

[⏪](#)

[⏩](#)

[◀](#)

[▶](#)

[Back](#)

[Close](#)

[Full Screen / Esc](#)

[Printer-friendly Version](#)

[Interactive Discussion](#)



Table 1. Comparison of the methane sources in the four simulations used in this study.

Input Data	TransCom	CN_a	CN_b	BGC
Anthropogenic Emissions	OB2001 ¹	0.72*OB2001	OB2001	OB2001
Wetland emissions	Ito and Inatomi, 2012	CLM4.0 ²	0.64*CLM4.0 ²	0.74*CLM4.5 ³
Rice paddy emissions	Ito and Inatomi, 2012	CLM4.0	CLM4.0	CLM4.5
Termite emissions	Fung et al. (1991)	Fung et al. (1991)	Fung et al. (1991)	Fung et al. (1991)
Fire emissions	GFED v2 ⁴	GFED v3	GFED v3	GFED v3

¹ OB2001 refers to the anthropogenic methane emissions in Olivier and Berdowski (2001).

² CLM4.0 refers to the methane emissions estimate in the CLM4.0 model as used in Meng et al. (2012).

³ CLM4.5 refers to the methane emissions estimated in CLM4.5 model.

⁴ GFED indicates the Global Fire Emission Database.

Note: the global total averaged emissions for the study period used in the TransCom, CN_a, and CN_b, BGC are the same, but spatial distribution of methane emissions might be different.

Seasonal and inter-annual variability in wetland methane emissions

L. Meng et al.

[Title Page](#)

[Abstract](#)

[Introduction](#)

[Conclusions](#)

[References](#)

[Tables](#)

[Figures](#)

◀

▶

◀

▶

[Back](#)

[Close](#)

[Full Screen / Esc](#)

[Printer-friendly Version](#)

[Interactive Discussion](#)



Table 2. A list of stations used in this study.

Station Name	ID	Lat	Lon	Elevation (m)	Data Availability
South Pole	spo	−89.98	24.80° W	2810	Feb 1983–Current
Cape Grim	cgo	−40.68	144.68° E	94	Jan 1984–Current
Tutuila (Cape Matatula)	smo	−14.24	170.57° W	42	Apr 1983–Current
Ascension Island (UK)	asc	−7.92	14.42° W	54	May 1983–Current
Cape Kumukahi	kum	19.52	154.82° W	3	Apr 1983–Current
Mauna Loa	mlo	19.54	155.58° W	3397	May 1983–Current
Mt. Waliguan	wlg	36.28	100.90° E	3810	May 1991–Current
Tae-ahn Peninsula	tap	36.72	126.12° E	20	Mar 1991–Current
Niwot Ridge	nwr	40.05	105.59° W	3523	Jun 1983–Current
Mace Head (Ireland)	mhd	53.33	9.90° W	8	Jun 1991–Current
Cold Bay	cba	55.2	162.72° W	25	May 1983–Current
Barrow	brw	71.32	156.60° W	11	Jan 1986–Current
Zeppelinfjellet (Norway)	zep	78.9	11.88° E	475	May 1994–Current
Alert (Canada)	alt	82.45	62.52° W	210	Jun 1985–Current

Seasonal and inter-annual variability in wetland methane emissions

L. Meng et al.

Table 3. Comparison of the mean growth rate of atmospheric methane concentration in each simulation with observations.

StationID	lat	Obs	TransCom	CN_a	CN_b	BGC
spo	-89.98	4.61	6.11	5.05	3.62	6.44
cgo	-40.68	4.64	5.96	4.86	5.67	6.35
smo	-14.24	4.44	5.34	4.21	5.09	5.87
asc	-7.92	4.23	5.72	4.57	5.55	6.29
kum	19.52	3.75	4.21	3.37	4.12	5.46
mlo	19.53	3.95	4.37	3.46	4.28	5.59
wlg	36.28	4.39	4.3	3.27	4.37	6.34
tae	36.72	3.2	3.72	2.92	3.89	4.88
nwr	40.05	4.16	4.4	3.49	4.27	5.56
mhd	53.33	3.92	2.78	1.98	2.98	4.52
cba	55.20	3.77	3.97	3.31	3.81	6.2
brw	71.32	3.27	3.42	2.92	3.35	6.42
zep	78.90	3.42	0.92	-0.48	1.99	4.2
alt	82.45	4.6	3.67	3.08	3.65	5.47
Average		4.03	4.21	3.29	4.05	5.69

Title Page

Abstract

Introduction

Conclusions

References

Tables

Figures

◀

▶

◀

▶

Back

Close

Full Screen / Esc

Printer-friendly Version

Interactive Discussion



Seasonal and inter-annual variability in wetland methane emissions

L. Meng et al.

Table 4. Model performance statistics including the Root Mean Square Error (RMSE) and bias. Bias is calculated as the absolute deviation of the mean between model simulations and observations.

	N–S Gradients	Growth Rate				Interannual Variability			
		South Pole	Mauna Loa	Niwot Ridge	Alert	South Pole	Mauna Loa	Niwot Ridge	Alert
RMSE									
TransCom	25.92	5.41	3.55	2.44	11.65	10.47	8.28	7.35	8.69
CN_a	17.57	0.57	4.22	2.88	5.13	12.65	13.96	14.59	15.06
CN_b	5.39	0.59	5.74	4.19	6.06	11.32	12.1	11.88	12.03
BGC	69.62	0.67	7.78	6.81	30.88	8.88	13.97	10.89	14.18
Bias									
TransCom	0.26	0.58	0.3	0.22	−1.69	0.08	0.01	0.02	0.01
CN_a	0.17	0.03	0.05	0.29	−1.05	0.02	0.02	0.03	0.04
CN_b	0.02	0.07	0.06	0.34	−0.72	0.03	0.02	0.02	0.03
BGC	0.71	0.06	1.36	1.29	−3.13	0.01	0.02	0.02	0.04

[Title Page](#)[Abstract](#)[Introduction](#)[Conclusions](#)[References](#)[Tables](#)[Figures](#)[⏪](#)[⏩](#)[◀](#)[▶](#)[Back](#)[Close](#)[Full Screen / Esc](#)[Printer-friendly Version](#)[Interactive Discussion](#)

Seasonal and inter-annual variability in wetland methane emissions

L. Meng et al.

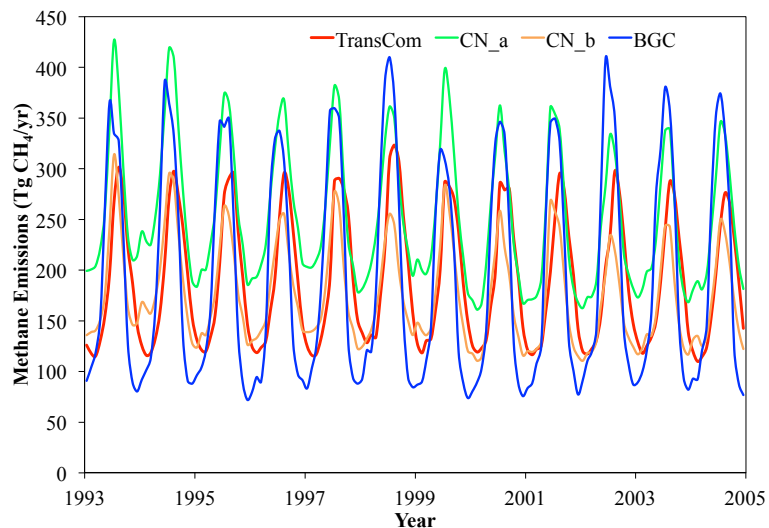


Figure 1. Comparison of the time series of combined methane emissions from wetlands and rice paddies used in the TransCom (Patra et al., 2011), CN_a, CN_b, and BGC experiments. Note that the average methane budget over the period of 1993–2004 is the same in the TransCom, CN_a, CN_b, and BGC experiments. CN_b is the reduced CN_a.

[Title Page](#)[Abstract](#)[Introduction](#)[Conclusions](#)[References](#)[Tables](#)[Figures](#)[◀](#)[▶](#)[◀](#)[▶](#)[Back](#)[Close](#)[Full Screen / Esc](#)[Printer-friendly Version](#)[Interactive Discussion](#)

Seasonal and inter-annual variability in wetland methane emissions

L. Meng et al.

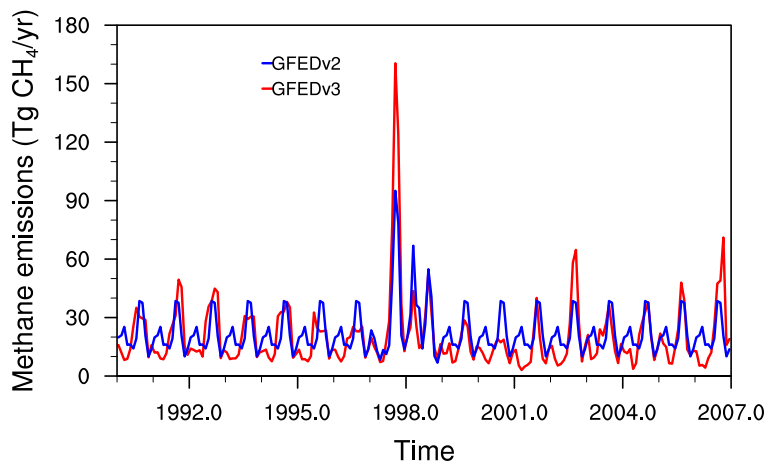


Figure 2. Comparison of the inter-annual variation in methane emissions from fire in the GFED v2 (van De Werf et al., 1996) and GFED v3 (Gilglio et al., 2010). These datasets are obtained from <http://www.globalfiredata.org/>.

[Title Page](#)[Abstract](#)[Introduction](#)[Conclusions](#)[References](#)[Tables](#)[Figures](#)[Back](#)[Close](#)[Full Screen / Esc](#)[Printer-friendly Version](#)[Interactive Discussion](#)

Seasonal and inter-annual variability in wetland methane emissions

L. Meng et al.

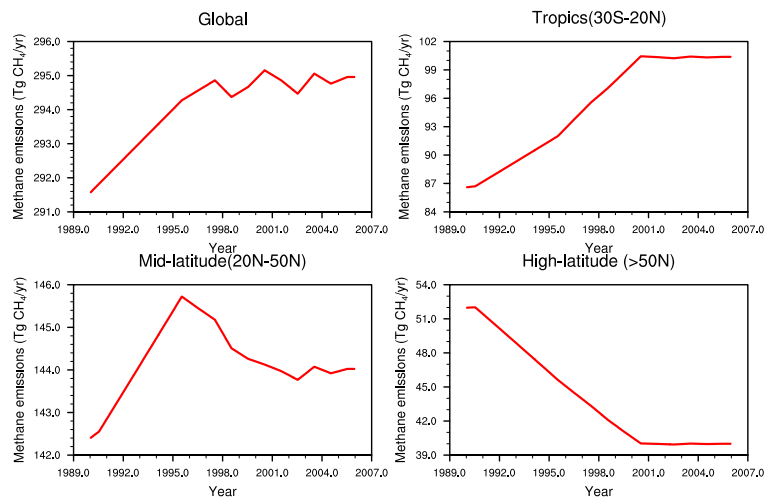


Figure 3. The inter-annual anthropogenic methane emissions in the globe, tropics, mid-latitude, and high-latitude. These datasets are obtained from TransCom (Patra et al., 2010).

Title Page

Abstract

Introduction

Conclusions

References

Tables

Figures

◀

▶

◀

▶

Back

Close

Full Screen / Esc

Printer-friendly Version

Interactive Discussion



Seasonal and inter-annual variability in wetland methane emissions

L. Meng et al.

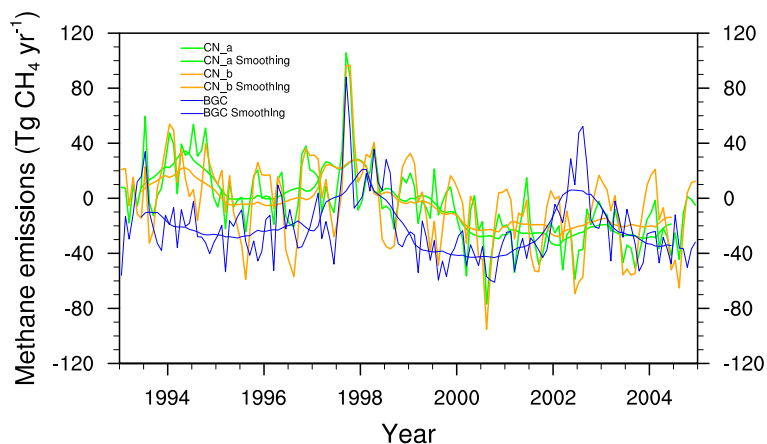


Figure 4. The difference in total emissions used in CN_a, CN_b, BGC experiments as compared with TransCom. A 12-month smoothing is also plotted for the difference of CN_a (CN_a – TransCom), CN_b (CN_b – TransCom), BGC (BGC – TransCom) with TransCom. Please note that the average of the difference in the period of 1993–2004 is zero.

Title Page

Abstract

Introduction

Conclusions

References

Tables

Figures

◀

▶

◀

▶

Back

Close

Full Screen / Esc

Printer-friendly Version

Interactive Discussion



Seasonal and inter-annual variability in wetland methane emissions

L. Meng et al.

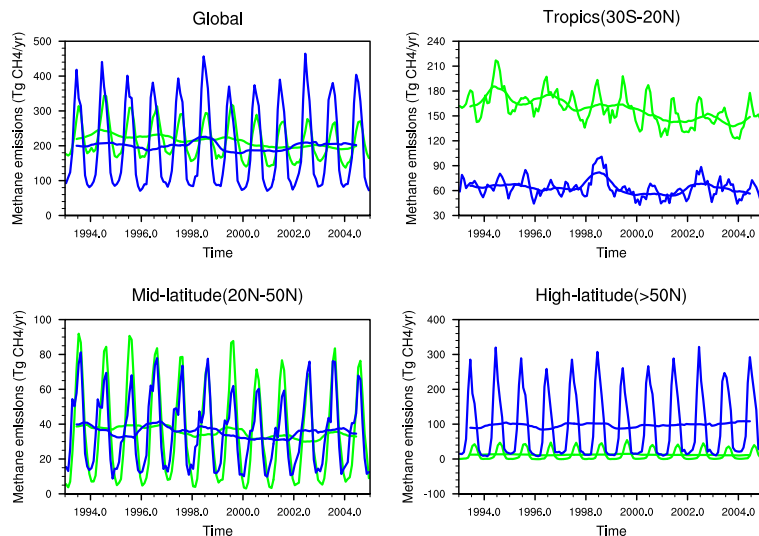


Figure 5. Temporal variation of wetland CH_4 fluxes estimated in CN_a (green) and BGC (blue). The globe is divided into three regions: Tropics (30°S – 20°N), Mid-latitude (20 – 50°N), and high-latitude ($> 50^\circ \text{N}$). Please note that this is the original methane emissions produced by CN_a and BGC without any multiplication. The smooth green and blue lines indicate the 12-month average wetland CH_4 fluxes for CN_a and BGC.

Title Page

Abstract

Introduction

Conclusions

References

Tables

Figures

◀

▶

◀

▶

Back

Close

Full Screen / Esc

Printer-friendly Version

Interactive Discussion



Seasonal and inter-annual variability in wetland methane emissions

L. Meng et al.

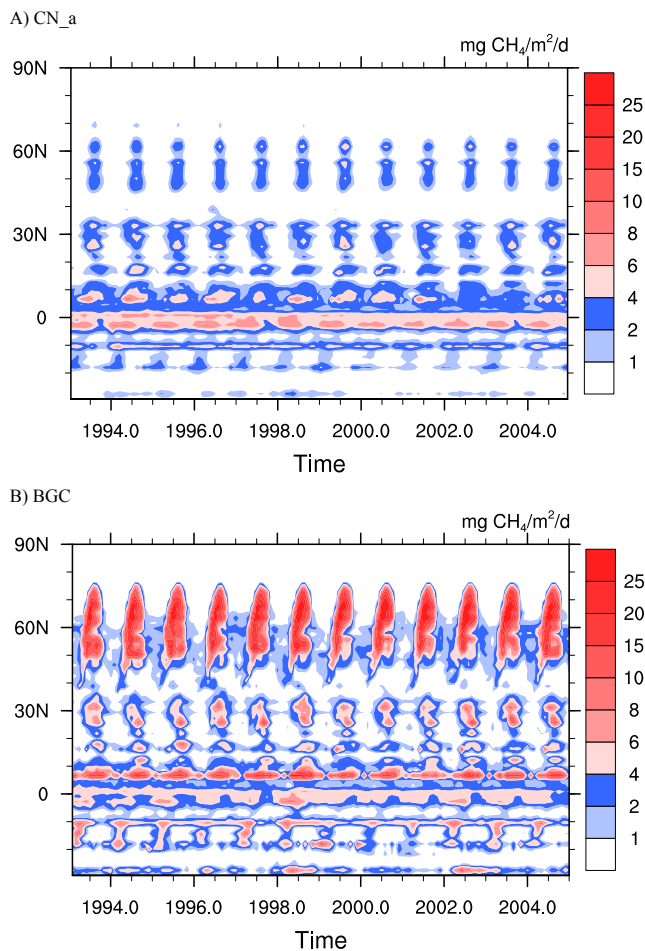


Figure 7. Zonal average monthly methane fluxes with time in CN_a (top, a) and BGC (bottom, b) experiments.

Seasonal and inter-annual variability in wetland methane emissions

L. Meng et al.

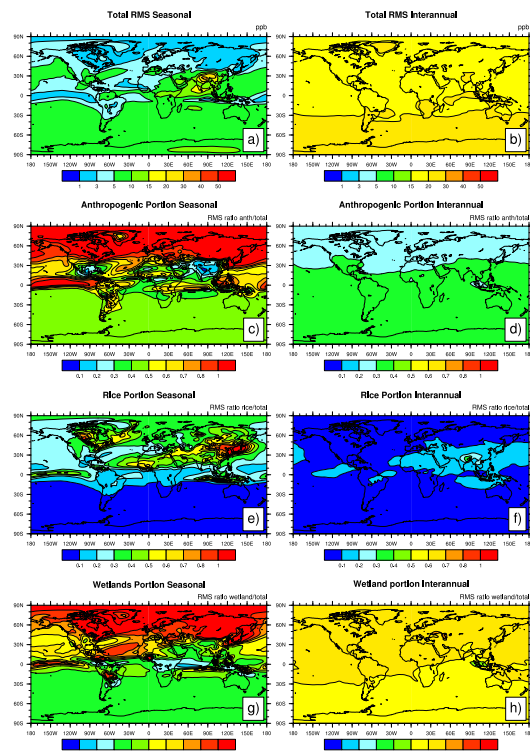


Figure 8. Absolute RMS variability (in ppb) from 1993–2004 of atmospheric CH_4 concentration in CN_a experiment. The left panel shows seasonal RMS variability and the right panel indicates inter-annual RMS variability. From the top to the bottom are total RMS variability, anthropogenic contribution to total RMS variability, rice contribution to total RMS variability, and wetland contribution to RMS variability. Note that portional RMS variability of anthropogenic sources, rice paddies, and wetlands add up to > 1 when cancellation among component tracers occurs in the summing of total CH_4 .

[Title Page](#)
[Abstract](#)
[Introduction](#)
[Conclusions](#)
[References](#)
[Tables](#)
[Figures](#)
[Back](#)
[Close](#)
[Full Screen / Esc](#)
[Printer-friendly Version](#)
[Interactive Discussion](#)

Seasonal and inter-annual variability in wetland methane emissions

L. Meng et al.

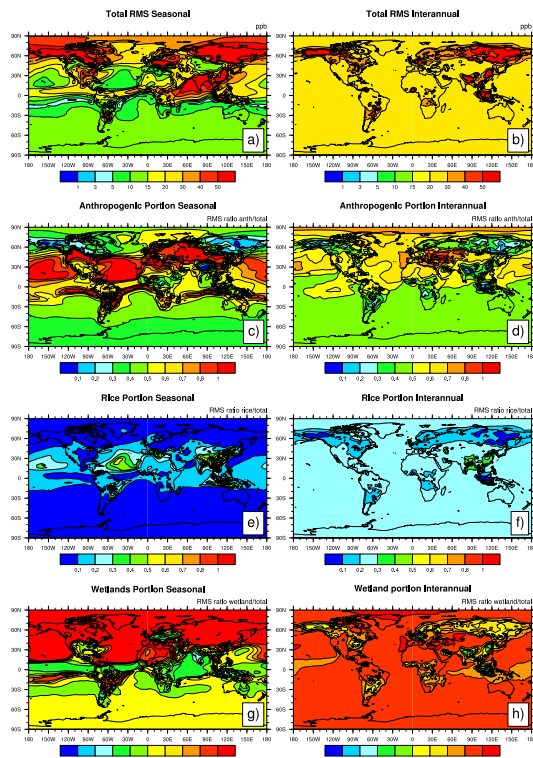


Figure 9. Absolute RMS variability (in ppb) from 1993–2004 of atmospheric CH_4 concentration in BGC experiment. The left panel shows seasonal RMS variability and the right panel indicates inter-annual RMS variability. From the top to the bottom are total RMS variability, anthropogenic contribution to total RMS variability, rice contribution to total RMS variability, and wetland contribution to RMS variability. Note that portional RMS variability of anthropogenic sources, rice paddies, and wetlands add up to > 1 when cancellation among component tracers occurs in the summing of total CH_4 .

[Title Page](#)
[Abstract](#)
[Introduction](#)
[Conclusions](#)
[References](#)
[Tables](#)
[Figures](#)
[⏪](#)
[⏩](#)
[◀](#)
[▶](#)
[Back](#)
[Close](#)
[Full Screen / Esc](#)
[Printer-friendly Version](#)
[Interactive Discussion](#)


Seasonal and inter-annual variability in wetland methane emissions

L. Meng et al.

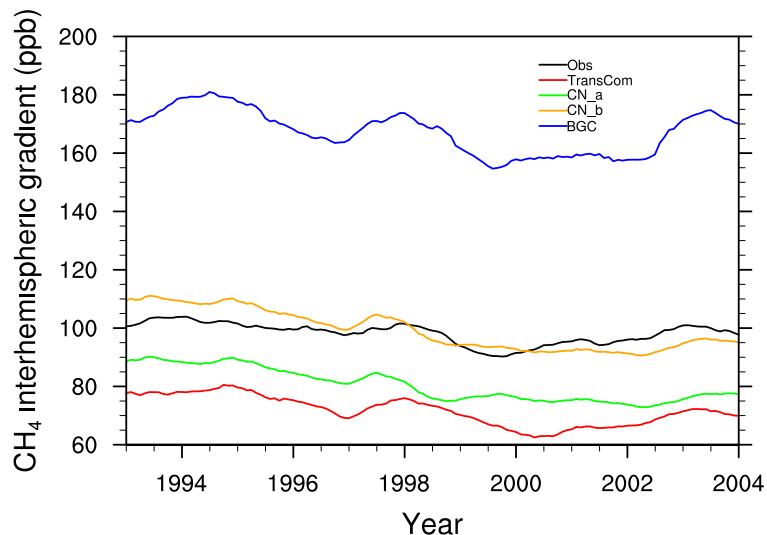


Figure 10. The interhemispheric gradients (N–S) in atmospheric CH₄ concentration. The N–S gradients are calculated as the difference in atmospheric CH₄ concentration in Northern and Southern Hemispheres at these stations listed in Table 1. The observational CH₄ concentration dataset at these stations is from the World Data Centre for Greenhouse Gases (WDCGG) at <http://ds.data.jma.go.jp/gmd/wdcgg/>.

Title Page

Abstract

Introduction

Conclusions

References

Tables

Figures

◀

▶

◀

▶

Back

Close

Full Screen / Esc

Printer-friendly Version

Interactive Discussion



Seasonal and inter-annual variability in wetland methane emissions

L. Meng et al.

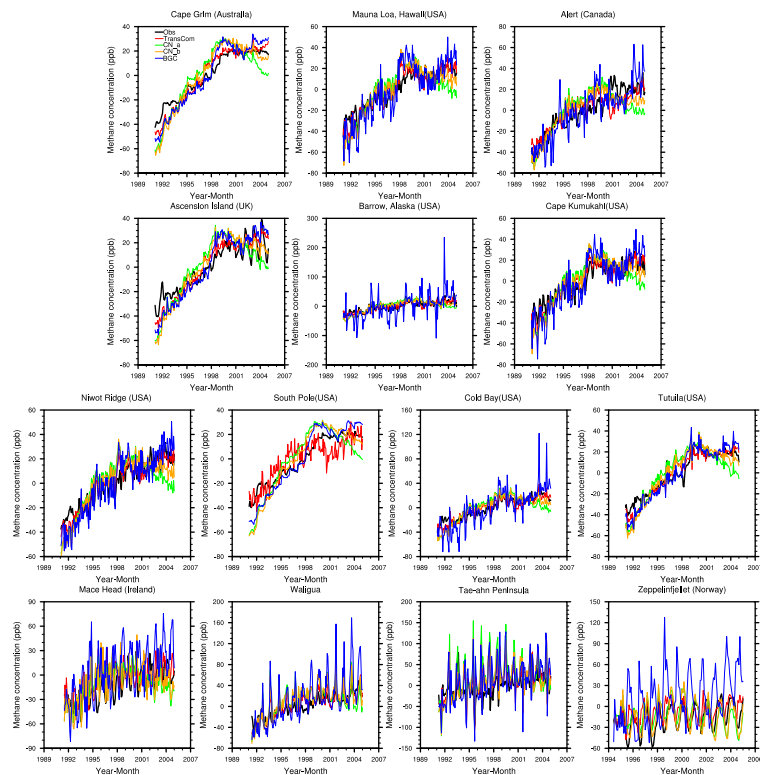


Figure 11. The comparison of model simulated atmospheric CH_4 concentration at closest grid box vs. observations. The climatological monthly mean is removed to focus on inter-annual variability in atmospheric CH_4 concentration at these stations. Model simulations are obtained from TransCom, CN_a, CN_b, and BGC experiments. The observational CH_4 concentration dataset at these stations is from the World Data Centre for Greenhouse Gases (WDCGG) at <http://ds.data.jma.go.jp/gmd/wdogg/>.

Title Page

Abstract

Introduction

Conclusions

References

Tables

Figures



Back

Close

Full Screen / Esc

Printer-friendly Version

Interactive Discussion



Seasonal and inter-annual variability in wetland methane emissions

L. Meng et al.

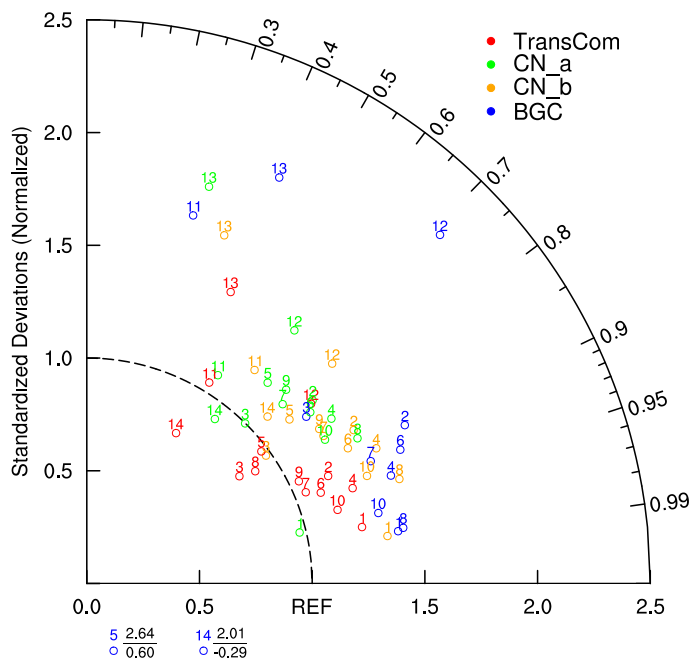


Figure 12. Taylor diagrams comparing the model inter-annual variability to methane observations at 14 stations. In this Taylor diagram, the angle from the x axis is the correlation coefficient between model and observed time series of atmospheric CH₄ concentration. The value on the radial axis is the ratio of standard deviation: $\sigma_{\text{model}}/\sigma_{\text{obs}}$. It represents the match between the amplitude of the model and observed inter-annual variability.

Title Page

Abstract Introduction

Conclusions References

Tables Figures

◀ ▶

◀ ▶

Back Close

Full Screen / Esc

Printer-friendly Version

Interactive Discussion



Seasonal and inter-annual variability in wetland methane emissions

L. Meng et al.

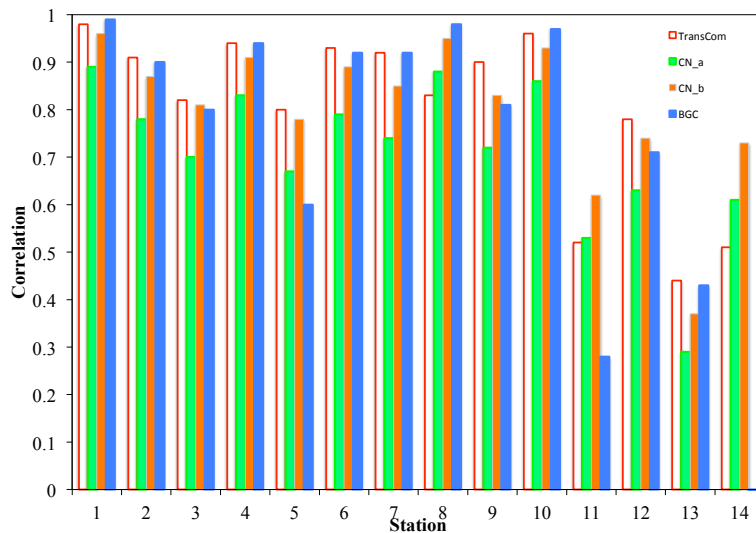


Figure 13. Comparison of correlations between TransCom, CN_a, CN_b, BGC and observations (same as in Fig. 12).

Title Page

Abstract

Introduction

Conclusions

References

Tables

Figures



Back

Close

Full Screen / Esc

Printer-friendly Version

Interactive Discussion



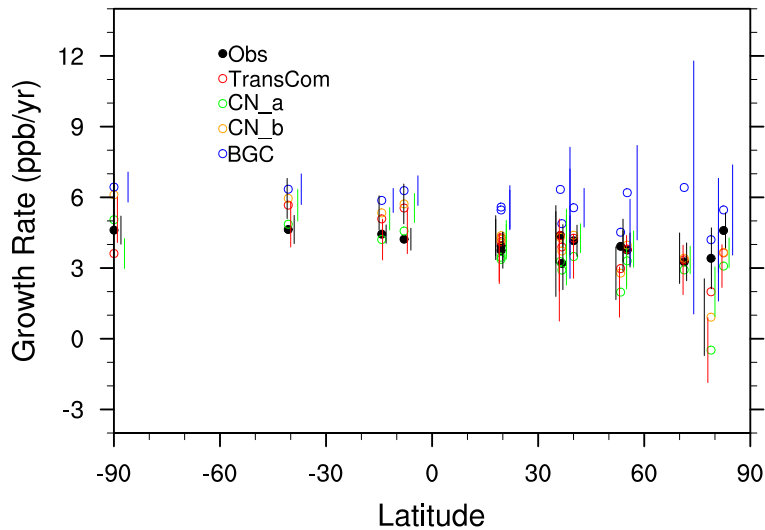


Figure 14. Atmospheric CH₄ growth rate as a function of latitude in observations, TransCom, CN_a, CN_b, and BGC simulations. 90 % confidence intervals are also shown.

Seasonal and inter-annual variability in wetland methane emissions

L. Meng et al.

Title Page	
Abstract	Introduction
Conclusions	References
Tables	Figures
⏪	⏩
◀	▶
Back	Close
Full Screen / Esc	
Printer-friendly Version	
Interactive Discussion	



Seasonal and inter-annual variability in wetland methane emissions

L. Meng et al.

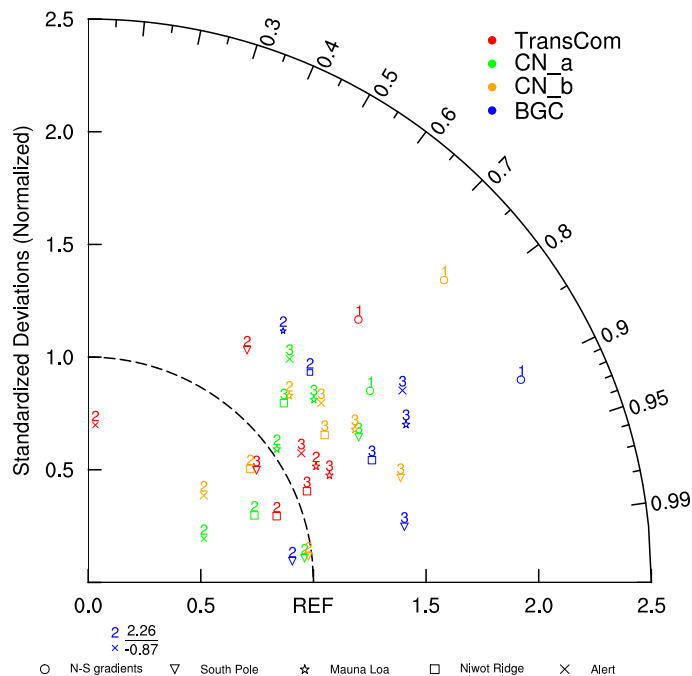


Figure 15. Taylor diagram comparing model N–S gradients (1), annual growth rates (2), and interannual variability (3) with observations for the South Pole, Mauna Loa, Niwot Ridge, and Alert (Canada) stations, respectively for the four simulations. The four stations are selected to represent the South Pole, tropics, mid-latitudes, and high latitudes. The annual growth rate is calculated as the difference between this year and previous year’s mean methane concentration. The N–S gradients are from Fig. 10.

Title Page

Abstract

Introduction

Conclusions

References

Tables

Figures



Back

Close

Full Screen / Esc

Printer-friendly Version

Interactive Discussion



Seasonal and inter-annual variability in wetland methane emissions

L. Meng et al.

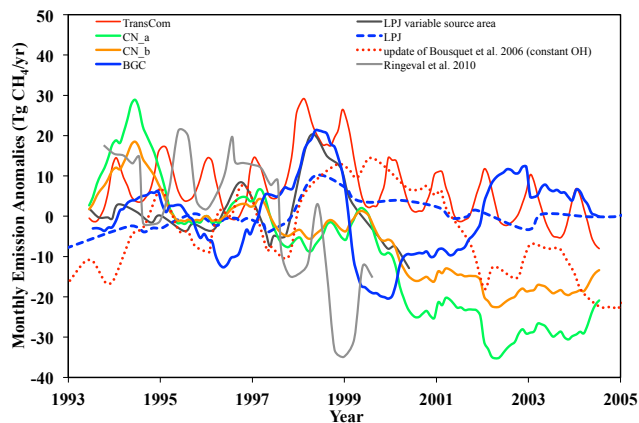


Figure 16. Comparison of the inter-annual variability in wetland CH_4 emissions used in this study and in others. A centered 12-month running mean filter has been applied to smooth monthly output. Data for “LPJ variable source area”, “LPJ”, and “update of Bousquet et al. 2006 (constant OH)” are obtained from Spahni et al. (2011). “LPJ variable source area” indicates emissions anomalies for 1993–2000 calculated by using the observed monthly inundated area (Prigent et al., 2007). “LPJ” indicates global CH_4 emission anomalies simulated by LPJ (natural ecosystem and rice agriculture) for scenario SC2 listed on Spahni et al. (2011). “update of Bousquet et al. 2006 (constant OH)” refers to global wetland emission anomalies derived from long-term atmospheric synthesis inversion updated from Bousquet et al. (2006). TransCom refers to emission anomalies derived from the combined wetland and rice paddies emissions. Methane emissions in Ringeval et al. (2010) are estimated using the ORCHIDEE global vegetation model with a process-based wetland CH_4 emission model. The wetland area is prescribed to the observed monthly-inundated area (Prigent et al., 2007) in Ringeval et al. (2010). Please note that in this figure, “LPJ variable source area”, “LPJ”, and “update of Bousquet et al. 2006 (constant OH)” data are obtained from Spahni et al. (2011). The mean anomalies over 1993–2000 are adjusted to zero for the all data plotted on this graph.

Title Page

Abstract

Introduction

Conclusions

References

Tables

Figures

◀

▶

◀

▶

Back

Close

Full Screen / Esc

Printer-friendly Version

Interactive Discussion



Seasonal and inter-annual variability in wetland methane emissions

L. Meng et al.

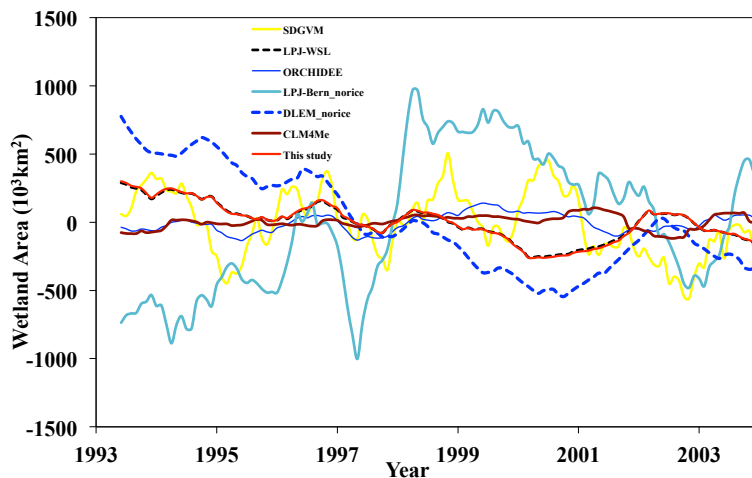


Figure 17. 12-month smoothing of the anomalies in wetland areal extents used in the models that participate in WETCHIMP project (Melton et al., 2013; Wania et al., 2013) and in this study (satellite inundated area obtained from Prigent et al., 2007 and Papa et al., 2010). LPJ-Bern_norice and DLEM_norice are LPJ-Bern and DLEM models that do not include rice paddy simulations, respectively. These notifications indicate WETCHIMP project also produce simulations with rice and only no rice simulations are included in this comparison study. In this figure, the long-term mean (1993–2004) is removed from each dataset.

Title Page

Abstract

Introduction

Conclusions

References

Tables

Figures

◀

▶

◀

▶

Back

Close

Full Screen / Esc

Printer-friendly Version

Interactive Discussion



Seasonal and inter-annual variability in wetland methane emissions

L. Meng et al.

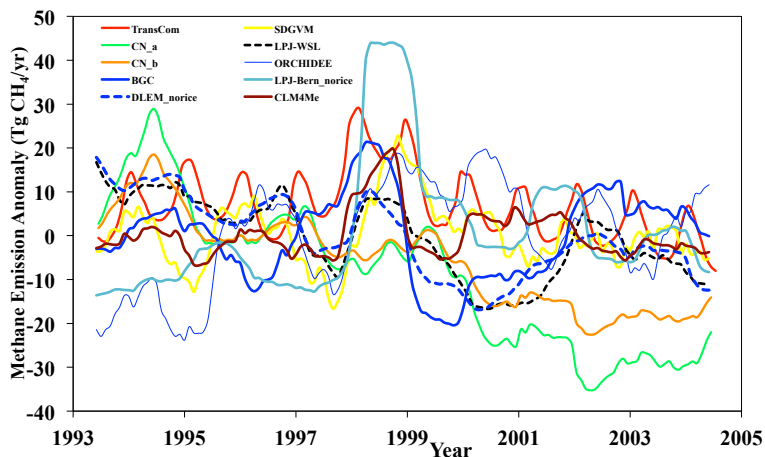


Figure 18. Similar to Fig. 16, but for the models that participate in WETCHIMP (Melton et al., 2013; Wania et al., 2013). Each model uses a different wetland extent to estimate methane emissions (see Table 1 in Melton et al., 2013 for wetland determination scheme in each model). LPJ-WSL prescribes wetland area from monthly inundation dataset (Prigent et al., 2007; Papa et al., 2010). DLEM_norice prescribes the maximum wetland area from the inundation dataset with simulated intra-annual dynamics. SDGVM uses the internal hydrological model to determine wetland locations. All other models parameterize wetland areas based on inundation dataset or land cover dataset that produce different inter-annual and intra-annual variability in wetland area. Please also refer to Melton et al. (2013) for detailed description of each model (SDGVM, LPJ-WSL, ORCHIDEE, LPJ-Bern_norice, DLEM_norice, CLM4Me).

Title Page

Abstract

Introduction

Conclusions

References

Tables

Figures

◀

▶

◀

▶

Back

Close

Full Screen / Esc

Printer-friendly Version

Interactive Discussion



Seasonal and inter-annual variability in wetland methane emissions

L. Meng et al.

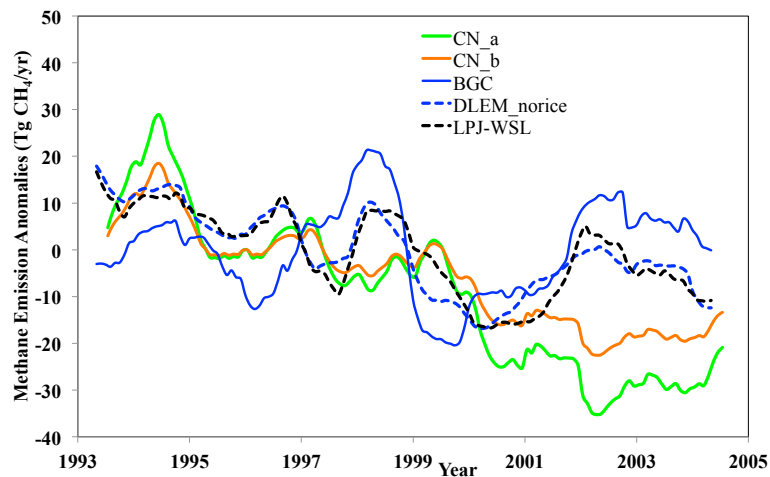


Figure 19. Comparison of methane emission anomalies in CN_a, CN_b, BGC, DLEM_norice, and LPJ-WSL. The anomalies are calculated by removing long-term average methane emissions during the period of 1993–2004.

[Title Page](#)[Abstract](#)[Introduction](#)[Conclusions](#)[References](#)[Tables](#)[Figures](#)[◀](#)[▶](#)[◀](#)[▶](#)[Back](#)[Close](#)[Full Screen / Esc](#)[Printer-friendly Version](#)[Interactive Discussion](#)

Seasonal and inter-annual variability in wetland methane emissions

L. Meng et al.

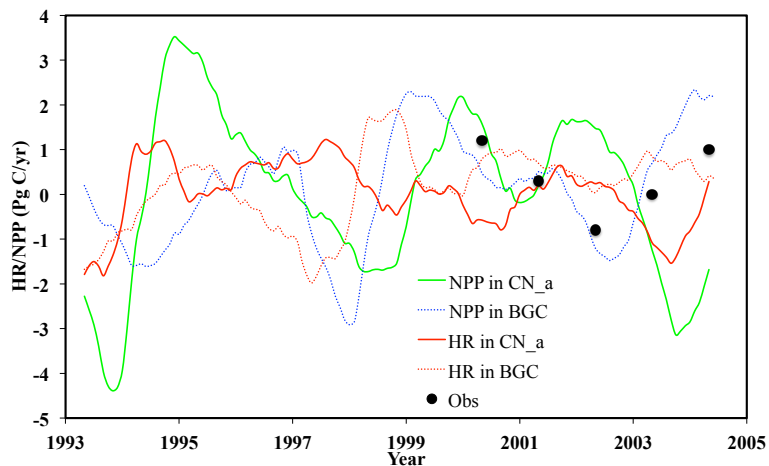


Figure 20. Temporal variation of the anomalies in globally averaged heterotrophic respiration (HR) and net primary production (NPP) in CN_a and BGC experiments. Blue dots indicate globally averaged NPP anomalies from satellites obtained from Zhao and Running (Zhao and Running, 2010).

Title Page

Abstract

Introduction

Conclusions

References

Tables

Figures

◀

▶

◀

▶

Back

Close

Full Screen / Esc

Printer-friendly Version

Interactive Discussion

